



Full-Length Research Article

Characteristics of Polyurethane Cross-Laminated Timber Made from a Combination of Pine and Coconut

Muhammad Iqbal Adi Baskara¹, Yusuf Sudo Hadi^{1*}, Muhammad Adly Rahandi Lubis^{2,**}, Muhammad Iqbal Maulana², Rita Kartika Sari¹, Fauzi Febrianto¹, Wahyu Hidayat³

¹ Department of Forest Products, Faculty of Forestry and Environment, IPB University. Jl. Ulin, Kampus IPB Darmaga Bogor, 16680, Bogor, Indonesia

² Research Center for Biomass and Bioproducts, National Research and Innovation Agency. Jl. Raya Jakarta-Bogor Km. 46, Cibinong, Bogor, 16911, Indonesia

³ Department of Forestry, Faculty of Agriculture, University of Lampung. Jl. Sumantri Brojonegoro 1, Bandar Lampung, 35145, Indonesia

* Corresponding Author. E-mail address: yshadi@indo.net.id

**Corresponding Author. E-mail address: marl@biomaterial.lipi.go.id

ARTICLE HISTORY:

Received: 13 January 2023

Peer review completed: 14 May 2023

Received in revised form: 22 May 2023

Accepted: 5 June 2023

KEYWORDS:

Coconut trunk

Cross-laminated timber

Layer combination

Pine wood

Polyurethane adhesive

ABSTRACT

The objective of this study was to assess the properties of cross-laminated timber (CLT) fabricated from the combination of Sumatran pine (P) and coconut trunk (C) bonded with polyurethane adhesive. The basic properties of raw materials and adhesives were characterized. The CLT panels' length, width, and thickness are 100 cm by 30 cm by 3.6 cm, respectively. Three-layer CLT was made with 4 combinations of face/core/back lamina, i.e., PPP, CCC, PCP, and CPC, which are arranged perpendicular to each other. The laminae were bonded using PU adhesive on 160 g.m⁻² glue spread. The CLT's delamination and wood failure percentages (WFP) were assessed following the JAS 3079 (2019) standard. The study's results demonstrated that the PU adhesive employed in this investigation could curl ideally at 30°C for 200 min. Solid pine and coconut's physical and chemical characteristics differed, but their wettability to polyurethane adhesives was identical. Hybrid pine CLT has greater attributes compared to single pine CLT. Single coconut CLT, on the other hand, offers better features than hybrid coconut CLT. All CLT samples failed to fulfil the JAS 3079 (2019) requirement for delamination ($\leq 10\%$) and WFP ($\geq 90\%$).

© 2023 The Author(s). Published by Department of Forestry, Faculty of Agriculture, University of Lampung. This is an open access article under the CC BY-NC license: <https://creativecommons.org/licenses/by-nc/4.0/>.

1. Introduction

Cross-Laminated Timber (CLT) is a mass-produced and widely used engineered wood. The CLT development began in the early 1990s with the partnership of industry and academia and was driven by the sawmill industry's necessity to use sideboards (Karacebeyli and Douglas 2013). In recent decades, the use of CLT has changed from small residential buildings to medium and high-rise buildings (Bahmanzad et al. 2020). The CLT production increased by 2.8 million m³ in 2019 (UNECE/FAO 2020). CLT panels are generally produced from softwood species (Aicher et al. 2016; Brandner et al. 2016; Marko et al. 2016; Sanjaya and Tobing 2019; Wang et al. 2017; Zhou et al. 2020). Softwood CLT panels in Indonesia can utilize wood from industrial plantation forests so that raw materials are easily obtained (Lestari 2017). One wood species that can be used as raw material is Sumatran pine (*Pinus merkusii*).

Sumatran pine fulfills the criteria to be the main ingredient for making CLT because it has a specific gravity of 0.49-0.61 (Febrianto et al. 2021), while the standards (ANSI 2018) require a CLT specific gravity of 0.35. Sumatran pine is classified as softwood, a fast-growing species that can be cut when small in diameter. Several studies on Sumatran pine used as CLT have good characteristics because one of the advantages of CLT is that it has good dimensional stability and increases strength, hardness, and mechanical properties (Lestari 2017). According to Hematabadi et al. (2020), arranging the center of the lamina on CLT with species with better specific gravity and mechanical properties would be of higher quality. Wood with this type of palmwood can also compete with softwood wood in manufacturing CLT. One example of palmwood that can be used as CLT is coconut (*Cocos nucifera*).

Coconut trunk is one of the building materials that can compete with other wood, is ready to obtain, has artistic motifs, and has high durability (Kusyanto 2015). According to Srivaro et al. (2020), coconut wood has dimensional stability, mechanical properties, and insulation equivalent to or better than the structural wood used in standard CLT panels. Coconut has a specific gravity ranging from 0.25-0.95 (Rangkang 2016; Srivaro et al. 2020). Thus coconut wood is often used as roof trusses, frames, doors, windows, floors, wall coverings, and even for structures such as poles or pillars and gazebos (Indrosaptono et al. 2018; Wijayanti 2014). Coconut meets the requirements for raw materials for making CLT (ANSI 2018). Therefore, pine and coconut are suitable for making CLT based on the above statement.

The adhesive is one factor that plays an essential role in manufacturing CLT. Polyurethane (PU) is one of the adhesives that can be used for CLT (Karacebeyli and Douglas 2013). Polyurethane (PU) adhesives are commonly used to manufacture CLT in Europe because they are free from solvents and formaldehyde emissions (Hasburgh et al. 2016). In addition, CLTs that use PU adhesive have better mechanical properties in shear strength than those using other synthetic adhesives, such as PRF (Sikora et al. 2016). This study aimed to assess the characteristic of CLT made from a combination of pine wood and coconut trunk. This study also examined the characteristics of the PU adhesive that will be used to make CLT.

2. Materials and Methods

2.1. Materials

Twenty-five-year-old Sumatran pine wood (*Pinus merkusii*) was provided by Gunung Walat University Forest, Sukabumi, Indonesia, and thirty-year-old coconut (*Cocos nucifera*) trunks were obtained from Bogor, Indonesia. Two-component PU adhesives were purchased from PT. Anugerah Raya Kencana, Banten, Indonesia. The PU adhesives consisted of methylene diphenyl isocyanate (MDI) and polyol.

2.2. Polyurethane Characterization

Polyurethane (PU) adhesives were prepared using isocyanates:polyol with a ratio of 1.8:1.0 (Kong et al. 2011). The adhesive was tested for its characteristics such as solids content, gelation time, viscosity, functional group analysis, Dynamic Mechanical Analysis (DMA), and Pyrolysis Gas Chromatography and Mass Spectroscopy (Py-GC/MS).

2.2.1. Solids content

Approximately 1 g of adhesive was weighed on an aluminium foil container and then placed in an oven at a temperature of $103 \pm 3^\circ\text{C}$ for 3 h. After that, the aluminium foil container was weighed. The solids content was determined using Equation 1.

$$\text{Solid content (\%)} = \frac{(WA-WE)}{(WB-WE)} \times 100\% \quad (1)$$

where WA is the weight of the PU sample and aluminium foil container after drying (g), WB is the weight of the PU sample and aluminium foil container before drying (g), and WE is the weight of the aluminium foil container only (g).

2.2.2. Gelation time

The PU adhesive sample was placed into a gel time meter tube (Techne GT-6, Colepalmer, USA). Furthermore, the time necessary for the gelatinization adhesive from the liquid phase was observed at 25°C . The gelation time was obtained when the timer stopped automatically.

2.2.3. Viscosity

The isocyanates, polyols, and PU adhesive samples were put into a measuring cup and placed on the rotational rheometer (RheolabQC, AntonPaar, Austria). The average viscosity was measured at rotating speeds of 50/s, 100/s, and 150/s at 25°C using spindle CC no. 27. Dynamic viscosity was measured for 200 min.

2.2.4. Functional group analysis

Functional group analysis was performed using Fourier Transform InfraRed (FTIR SpectrumTwo, Perkin Elmer, USA) for the liquid and solid adhesives using Universal Attenuated Total Reflectance (UATR) method. Samples of isocyanate, polyol, and PU adhesive were placed in a sample holder, pressed, and scanned from $400\text{-}4000\text{ cm}^{-1}$ with an average of 16 scans on resolution 4 cm^{-1} .

2.2.5. Dynamic mechanical analysis (DMA)

Samples were prepared by spreading 160 g.m^{-2} of PU adhesive on filter paper and then air-dried. Dynamic mechanical analysis measurements (DMA 8000, Perkin Elmer, USA) were carried out in dual cantilever mode at $25\text{-}60^\circ\text{C}$ with a constant frequency of 1 Hz. The viscoelastic response is expressed in storage modulus (E) and damping ability ($\tan \delta$) at a $2^\circ\text{C}/\text{min}$ heating rate. Isothermal mechanical analysis was carried out at 25°C for 200 min.

2.2.6. Pyrolysis gas chromatography and mass spectroscopy (Py-GC/MS)

Chemical compound analysis was performed using Py-GC/MS (QP-2020 NX Shimadzu, Japan) instrument. About 5 g of PU adhesive was dropped into an eco-cup. The adhesive was then pyrolyzed using EGA/PY-3030D multi-shot pyrolysis for 0.1 min at 500°C in helium as the carrier gas. The pressure was set to 20.0 kPa (15.9 mL/min and column flow 0.61 mL/min). Before being escalated at a heating rate of $10^\circ\text{C}/\text{min}$ to 300°C , the temperature was held for 1 min at 50°C . The

temperature was maintained at 300°C for 13 min. The program was obtained using the Py-GCMS program (NIST LIBRARY 2017, Shimadzu, USA).

2.3. Characterization of Raw Materials

2.3.1. Physical and chemical properties

The physical characteristic of pine and coconut, such as density, moisture content (MC), and volume shrinkage, were determined according to the ASTM D-143:2014 standard (ASTM 2014). The chemical characteristics of pine and coconut, such as extractive content, and pH, were determined according to the TAPPI standard (TAPPI 1991).

2.3.2. Surface roughness and wettability

Surface roughness measurement uses a surface roughness tester following the ISO 4287:1997 (ISO 1997). Measurements were taken at five different spots on the sample's surface perpendicularly to the fiber. Arithmetical Mean Roughness (Ra) was used as the surface roughness parameter.

Wettability was measured using the sessile drops method. An injection was used for dripping about 0.02 mL of adhesive onto the surface of the wood. The dripping process was recorded for 180 s of video and then split into image fragments at intervals of 10 s using GOM Player software. ImageJ Software equipped with the drop snake plugin was used to measure the contact angles of the droplet captured in the image fragments. The value of the contact angle constant was determined from the contact angle (θ) and the time (t) and using SAS 9.0. The K parameter value was calculated based on the S/G model (Shi and Gardner 2001) following the formula:

$$\theta = \frac{\theta_i \cdot \theta_e}{\theta_i + (\theta_e - \theta_i) \text{Exp}\left[K \left(\frac{\theta_e}{\theta_e - \theta_i}\right) t\right]} \quad (2)$$

where θ is the contact angle at a particular time, θ_i is the initial contact angle, θ_e is the equilibrium contact angle, t is time, and K is the contact angle constant.

2.4. Cross-Laminated Timber Manufacturing

Pine logs and coconut trunks were split into lamina with a thickness of 1.3 to 1.5 cm, then sawn to 100 cm in length and a width of 10 cm. The laminate was then air-dried until the moisture content reached air dry 15%. Next, the lamina was screened visually to identify defects. Sorting was done manually using a non-destructive method for grouping the lamina. The visual and technical separation were referred to JAS 3079 (2019). The sorted lamina was cut into 1.2 cm thickness and 30 cm in length as the center of the CLT.

PU adhesive was spread on the lamina with a glue spread of 160 g/m² (Liao et al. 2017). The laminae layers were arranged perpendicularly to form a 3-layer CLT (face-core-back) measuring 100 cm × 30 cm × 3.6 cm. The CLT layer was prepared in various ways based on the type of raw material (pine, coconut, and their combination). Next, the CLT was compressed at 30°C at a pressure of 0.8 MPa for 200 min which refers to the research of Liao et al. (2017), which stated that the polyurethane glue spread, pressure, and compressing time were the best for obtaining optimum block shear, failure percentage (FP), and rate of delamination values. The final form of

the CLT can be seen in **Fig. 1**. After compression, the CLT was conditioned for seven days at a relative humidity of 60% and a temperature of 30°C.



Fig 1. Cross-laminated timber ($100 \times 30 \times 3.6 \text{ cm}^3$).

2.5. Testing Procedures

Cross-laminated timber's physical and mechanical characteristics, such as density, moisture content, volume shrinkage, water adsorption, thickness swelling, delamination, modulus of elasticity (MOE), modulus of rupture (MOR), block shear strength, and wood failure percentage, were determined according to JAS 3079 (JAS 2019).

2.5.1. Density

The sample size of $7.5 \text{ cm} \times 7.5 \text{ cm} \times 3.6 \text{ cm}$ was measured to obtain the air-dried volume (V), and the weight of samples was then weighed to obtain air-dried weight (W). The density value was calculated using the following formula:

$$\text{Density (g.cm}^{-3}\text{)} = \frac{W}{V} \quad (3)$$

2.5.2. Moisture content

The initial weight of the sample was measured (W_1) and then dried at a temperature of $103 \pm 2^\circ\text{C}$ until reaching the constant weight, and the oven-dried weight (W_2) of the sample was measured immediately. The moisture content value was calculated using the following formula:

$$\text{Moisture content (\%)} = \frac{W_1 - W_2}{W_2} \times 100\% \quad (4)$$

2.5.3. Volume shrinkage

The sample dimension was measured to obtain the initial volume (V_1), then dried at $103 \pm 2^\circ\text{C}$ until the weight was constant. The oven-dried dimension of the samples was measured to obtain the volume (V_2). The volume shrinkage value was calculated using the following formula:

$$\text{Volume shrinkage (\%)} = \frac{V_1 - V_2}{V_2} \times 100\% \quad (5)$$

2.5.4. Water adsorption and thickness swelling

The sample's weight (W_1) and thickness (T_1) were measured for the calculation of water adsorption (WA) and thickness swelling (TS). The samples were immersed in water at room

temperature for 24 h. After immersing, the weight (W_2) and average thickness (T_2) were measured again. The WA and TS values were determined utilizing the following formula:

$$WA (\%) = \frac{W_2 - W_1}{W_1} \times 100\% \quad (6)$$

$$TS (\%) = \frac{T_2 - T_1}{T_1} \times 100\% \quad (7)$$

2.5.5. Cold water delamination

Delamination samples with dimensions of 7.5 cm × 7.5 cm × 3.6 cm size were soaked in water at ambient temperature for 24 h. The samples were then oven-dried at $70 \pm 3^\circ\text{C}$ until the constant weight was reached. The delaminated lengths at the glue line of all sides were measured immediately. The delamination value was calculated using the following formula:

$$\text{Delamination } (\%) = \frac{\Sigma \text{ Delaminated glue line}}{\Sigma \text{ Total glue line}} \times 100\% \quad (8)$$

2.5.6. Boiling water delamination

Delamination samples with 7.5 cm × 7.5 cm × 3.6 cm size were immersed for 4 h in boiling water. The samples were then soaked in water at ambient temperature for 1 h before being oven dried at $70 \pm 3^\circ\text{C}$ to a constant weight. The delamination value was calculated using the above formula.

2.5.7. MOE and MOR

Universal Testing Machine (UTM, Baldwin, USA) was utilized to evaluate the modulus of elasticity (MOE) and modulus of rupture (MOR) of the CLT. The span length was set to 76 cm, and the test was performed with a 14.7 MPa/min load speed until the failure of the sample. The MOE and MOR values were determined using the formulas below:

$$MOE (MPa) = \frac{\Delta PL^3}{4\Delta ybh^3} \quad (9)$$

$$MOR (MPa) = \frac{3PL}{2bh^2} \quad (10)$$

where ΔP is the difference in proportion limit between the maximum and minimum load (N), P is the maximum load (N), L is the span (mm), Δy is the difference in deflection between the top and bottom load (mm), b is the sample width (mm), and h is the sample thickness (mm).

2.5.8. Block shear strength

The parallel-to-grain with size 5.0 cm × 2.5 cm × 3.6 cm and the perpendicular-to-grain with size 4.0 cm × 5.0 cm × 3.6 cm were prepared for block shear strength samples. The sample was tested at a speed of 2 mm/min. The block shear strength value was calculated using the following formula:

$$\text{Block shear strength (MPa)} = \frac{P}{A} \quad (11)$$

where P is the maximum load when the sample breaks (N) and A is the residual bond area (mm^2).

2.6. Data Analysis

A completely randomized design was performed in the form of variations in the combination of layers (face-core-back) in the form of pine-pine-pine (PPP), coconut-coconut-coconut (CCC), pine-coconut-pine (PCP), and coconut-pine-coconut (CPC). Each treatment was applied in 3 repetitions. The factor effect on observations was observed at a 95% confidence level using the Analysis of Variance (ANOVA) F test. Duncan's Multiple Range Test (DMRT) was performed on parameters that showed a significant effect to determine the significant difference among treatments. The analyses were carried out using the IBM SPSS Statistics (Version 26, SPSS Inc., USA) software. The analysis results were compared to the JAS 3079 standards (JAS 2019).

3. Results and Discussion

3.1. Properties of Polyurethane Adhesive

The data in **Table 1** shows the solids content and gelatination time of PU 1.8. The solids content of PU 1.8 generated by isocyanate and polyol reaction is 97.37%. The solid content values were similar to the published work that reported PU adhesives could reach 100% solids content (Hass et al. 2012). An adhesive solid's content value depends on the constituent materials. Isocyanate and polyol had a solids content of 99.47% and 86.73%, respectively.

Table 1. Solid content and gelatination time of PU 1.8

Characteristics	Value
Solids content (%)	97.37 ± 0.42
Gelatination time at 25°C (min)	84.9

Gelation time is the time it takes for a liquid adhesive to gel at a given temperature. The gelation time of PU 1.8 at 25°C is around 84.9 min. This period is still within the long span of CLT compression employing an effective polyurethane adhesive, which is 200 min (Liao et al. 2017). The PU 1.8 adhesive is suitable for use in this investigation based on the solids content and gelation time criteria. The viscosity of PU 1.8 may also be used to establish its compatibility with the production of CLT.

Fig. 2 shows the difference in viscosity of isocyanates (a) and polyols (b) with PU 1.8 (c). The average viscosity of isocyanate and polyols were 200.29-212.38 mPa.s and 122.95-127.22 mPa.s, respectively. The resulting PU 1.8 has a viscosity range of 784.96-947.67 mPa.s. The viscosity of PU 1.8 is higher than isocyanate and polyol viscosity. Isocyanate and polyol had a constant viscosity, while the PU 1.8 decreased over time. It could result from an alteration in the properties of the functional groups depicted in **Fig. 3**. The viscosity of PU 1.8 adhesive was greater compared to the commercially available PU resin, with values ranging between 150 to 250 mPa.s. This is due to the molecular weight of PU 1.8 (NCO/OH ratio 1.8/1.0) being higher than the commercial PU adhesive (NCO/OH ratio 1.0/1.0). A similar trend was also reported for PU adhesives with NCO/OH ratios of 1.2/1.0 and 1.5/1.0 (Aisyah et al. 2023; Hariz et al. 2023). A higher molecular weight of a compound can increase its viscosity (Sur and Rothstein 2018).

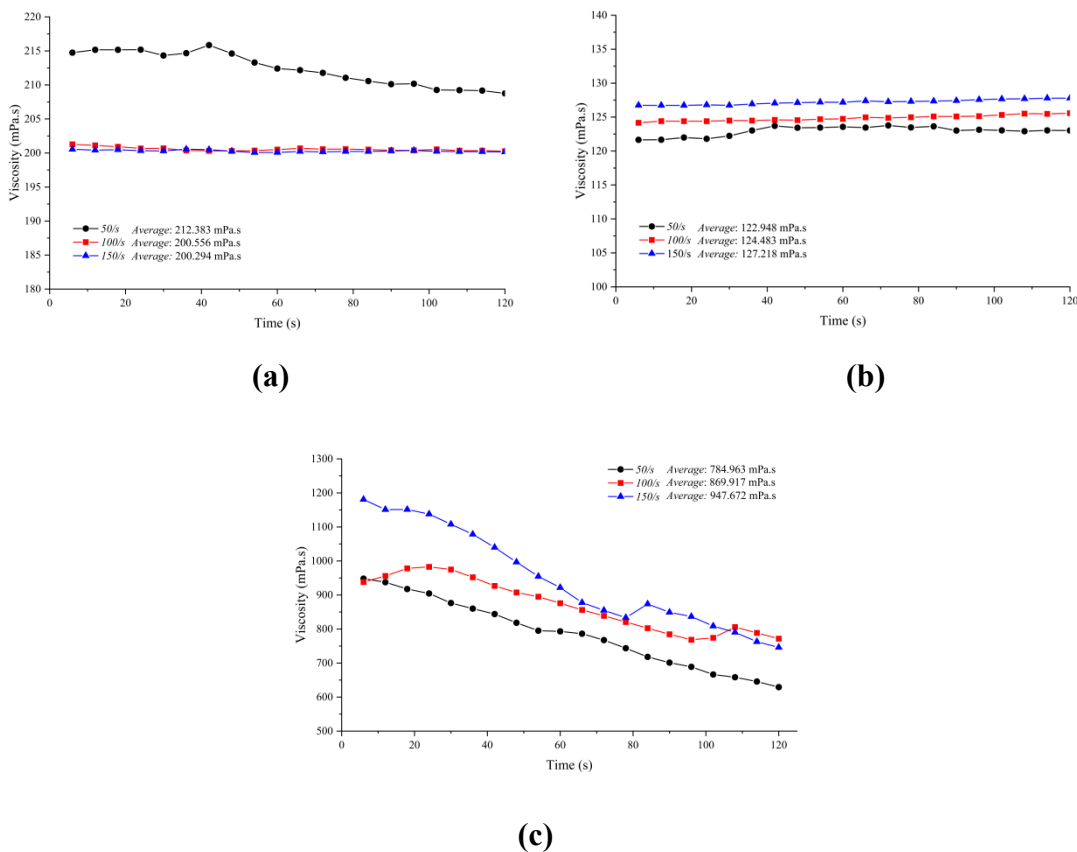


Fig. 2. The viscosity of isocyanate (a), polyol (b), and PU 1.8 (c).

3.1.1. Functional group analysis

Fig. 3 shows several liquid and solid PU functional groups, confirming the presence of isocyanate and polyol. This is shown from the peak at 2248 cm⁻¹ related to NCO, the peak at 1103 cm⁻¹ from the hydroxyl group (OH), at wavenumbers 1460-1600 cm⁻¹ which suggests the formation of bound urethane groups, and at numbers 1600-1720 cm⁻¹ of free urethane. Table 2 summarizes the functional groups in isocyanate, polyol, liquid PU, and solid PU.

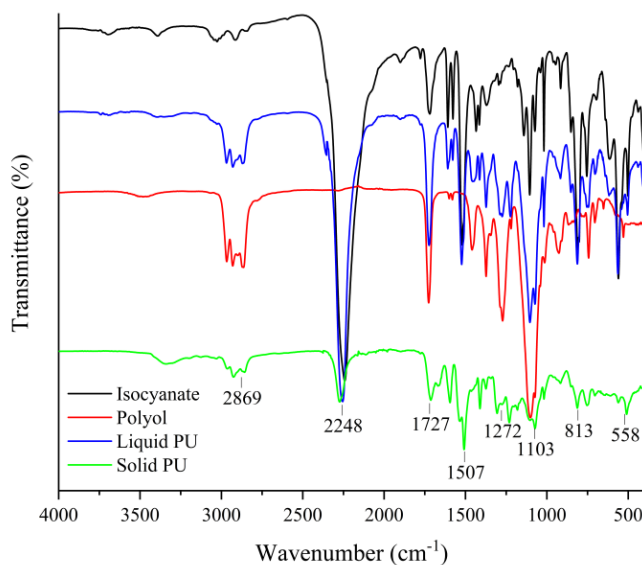


Fig. 3. FTIR spectra of isocyanate, polyol, and PU 1.8 in liquid and solid form based on the results of FTIR.

The highest peak in PU 1.8 was at 2248 cm^{-1} , which indicates the presence of $\text{N}=\text{C}=\text{O}$ groups, and 1103 cm^{-1} , which indicates the presence of secondary O-H groups (Lubis et al. It means there is still isocyanate that does not react with a polyol, which decreases its viscosity. On the other hand, the peak related to secondary O-H groups and $\text{N}=\text{C}=\text{O}$ in solid PU drops while retaining the peak of the urethane bond at 1507 cm^{-1} . It could be because PU 1.8 has thickened and lost a bond group, lowering its reactivity.

Table 2. Summary of FTIR analysis results of isocyanate, polyol, liquid, and solid PU 1.8

Wavenumber (cm^{-1})				Functional Group	References
Isocyanates	Polyols	PU Liquid	PU Solid		
2869	2869	2869	2869	C-H	2800-3000 cm^{-1} (Gurunathan et al. 2015)
2248	-	2248	2248	$\text{N}=\text{C}=\text{O}$	2230-2276 cm^{-1} (Oliviero et al. 2019; Poh et al. 2014)
1727	1727	1727	1727	C=O	1664-1780 cm^{-1} (Gurunathan et al. 2015)
1507	1507	1507	1507	Urethane bond	1460-1600 cm^{-1} (Hidayat et al. 2022; Thébault et al. 2015)
1272	1272	1272	1272	C-N (Amide II band)	1200-1500 cm^{-1} (Handika et al. 2021; Sunija et al. 2014)
1103	1103	1103	1103	Secondary O-H	1100-1200 cm^{-1} (Hazmi et al. 2013; Kong et al. 2011)

3.1.2. Dynamic mechanical analysis (DMA)

Fig. 4a shows the greatest E' of PU 1.8 value of 45.54 GPa at 27.93°C . It denotes the temperature of PU 1.8 with the best elasticity ability. **Fig. 4a** exhibits a drop in E' following the peak and a rise in the value of E'' . A high E'' value corresponds positively with the stiffness or viscosity of adhesive (Böhning et al. 2019; Sankar et al. 2011). The value of E' is the result of a measurement of stored energy and is highly dependent on the type of polymer and temperature, while E'' measures the energy lost from the specimen due to molecular friction that occurs in a viscous flow (Lubis et al. 2022; Park and Kim 2008). Furthermore, the rising trend of the tan graph, which reflects damping ability (Menard and Menard 1990), is also seen in **Fig. 4a**.

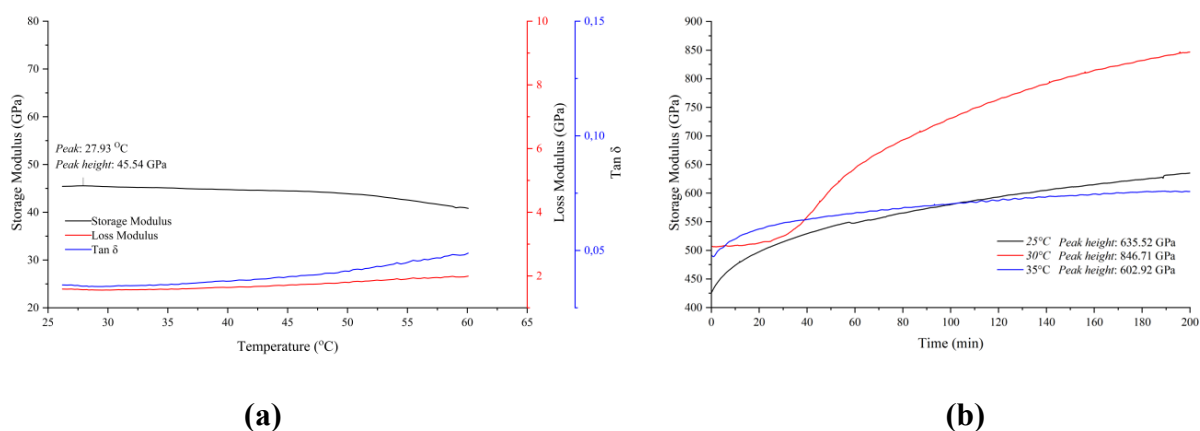


Fig. 4. Thermo-mechanical analysis responses of PU 1.8 in variations of time (a) and temperature (b).

The thermomechanical properties of PU molecules show the possibility of compaction at 1.8 over 27.93°C. Several other studies have experienced adhesive solidification that is too fast due to temperature that shortens the period of the penetration of liquid adhesive and the formation of mechanical bonds to wood (Bekhta et al. 2020; Lei and Frazier 2015). Applying the optimal pressing time of polyurethane-bonded CLT (Liao et al. 2017), the trend of E' of PU 1.8 with a temperature of 35°C for 200 min in Fig. 4(b) does not exhibit major fluctuations after ± 60 min. Nevertheless, the graph that continues to rise at 200 min implies a higher possibility for E' at > 200 min. Overall, PU 1.8 adhesive is characterized as a thermosetting adhesive that can penetrate and harden optimally at 35°C for 200 min.

3.1.3. Pyrolysis gas chromatography and mass spectrometer (Py-GC/MS)

Fig. 5 and Table 3 show the Py-GC/MS analysis results of PU adhesives. The peak with the highest intensity was spotted at 27.8 min, showing Methane-isocyanate compounds. At 24.8 min, the peak showed 3,3'-Diamino diphenylmethane compounds, and at 2.60 min showed Acetonitrile compounds.

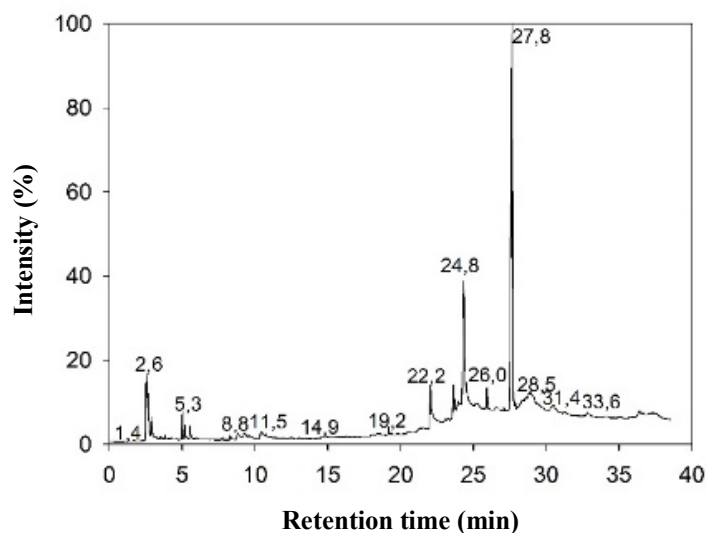
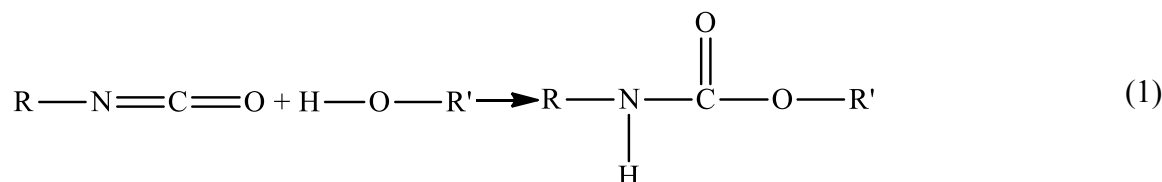
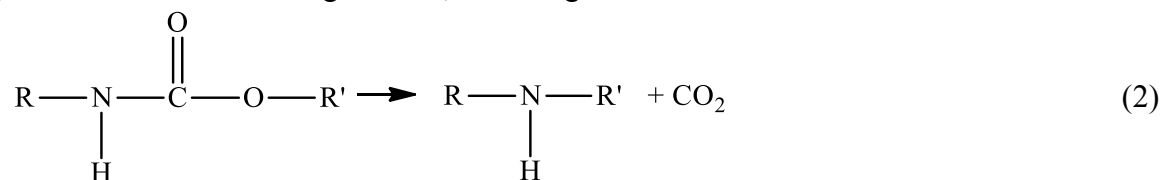


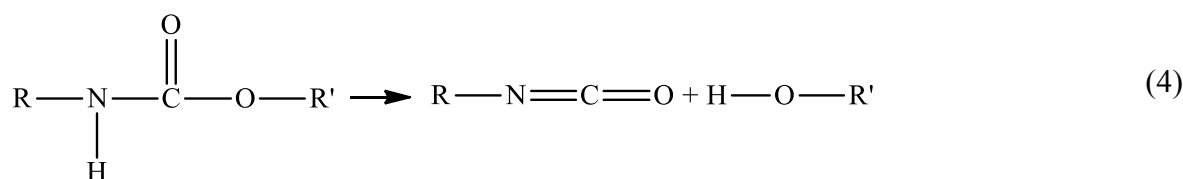
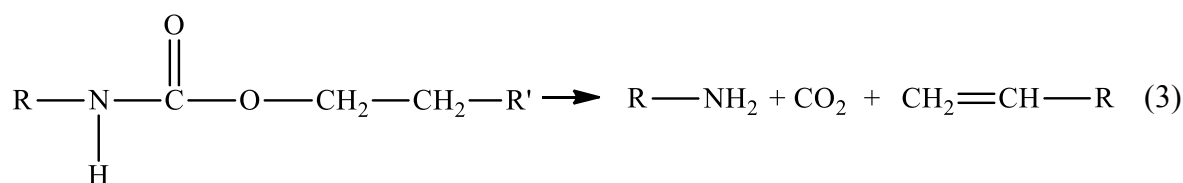
Fig. 5. Analysis of py-GC/MS results.

Polyurethane is formed and degraded as a result of Py-GC/MS. The formation reaction of polyurethane is as follows:



According to Scheme 1, the reaction of PU formation is characterized by peaks number 21, 25, 27, and 29 ($-\text{N}=\text{C}=\text{O}$) and peak number 30 ($-\text{OH}$), which form polyurethane with urethane along with several forms of degradation, including Scheme 2-4.





Peak numbers 21, 25, 27, and 29 ($-\text{N}=\text{C}=\text{O}$), and peak numbers 30 ($-\text{OH}$) represent polyurethane degradation product (Scheme 2). Peak numbers 3, 14, and 17 ($-\text{NH}_2$); peak numbers 2, 13, 15, and 22 (chain N); 4, 5, 6, 8, 9, 10, 11, 12, 18, 19, 20, 23, 26, and 28 ($-\text{NH}-$); peak numbers 7 and 16 ($\text{CH}_2=\text{CH}$); and peak number 1 ($\text{O}=\text{C}=\text{O}$) represents polyurethane degradation product (Scheme 3 and Scheme 4).

Table 3. Results of analysis py-GC/MS

Peak number	Retention (min)	Molecular weight (m/z)	Compound
1	2.52	44	Carbon dioxide
2	2.60	41	Acetonitrile
3	2.68	29	Methylene, 1-amino-
4	2.87		Ethylenimine
5	3.51	43	Ethylenimine
6	3.80		Ethylenimine
7	5.02	70	1-Pentene
8	5.18	45	Dimethylamine
9	5.51	43	Ethylenimine
10	8.29	45	Dimethylamine
11	19.18	105	Diethanolamine
12	22.04	43	Ethylenimine
13	22.26	55	Propanenitrile
14	23.64	198	3,3'-Diaminodiphenylmethane
15	23.94	55	Propanenitrile
16	23.98	70	1-Pentene
17	24.32	198	3,3'-Diaminodiphenylmethane
18	25.93	97	1H-Pyrrole-2,5-dione
19	27.08		Benzaetanamine, N, α -dimethyl-
20	27.64	149	Benzaetanamine, N, α -dimethyl-
21	27.84	57	Methane, isocyanato-
22	28.62	55	Propanenitrile
23	28.79	43	Ethylenimine
24	28.88	95	2(1H)-Pyridinone
25	28.93	57	Methane, isocyanato-
26	29.04	97	1H-Pyrrole-2,5-dione
27	29.14	57	Methane, isocyanato-
28	30.50	43	Ethylenimine
29	32.81	57	Methane, isocyanato-
30	36.39	96	3-Furaldehyde

Sources: (Dyer and Newborn 1958; Dyer and Read 1961; Dyer and Wright 1959; Zhang et al. 2009).

3.2. Properties of CLT Raw Materials

Table 4 shows the specific gravity, air-dried and kiln-dried density, moisture content, and volume shrinkage of pine wood and coconut trunk. Coconut trunk has a higher specific gravity and density than pine wood. Pinewood has a specific gravity of 0.50-0.52. These values are still in the range of pine wood in several other studies (Hadjib and Rachman 2009; Polosakan and Alhamd 2014). Coconut trunk has a specific gravity of 0.67. In other physical properties of wood studies, this value is still in the range of coconut trunk (Awaludin and Sutapa 2012). The specific gravity of pine wood and coconut trunk still fulfilled the raw material CLT standard of 0.35 (ANSI 2018). Air-dried and kiln-dried densities of heartwood pine were 0.53 and 0.54 g.cm⁻³, sapwood pine was 0.51 and 0.50 g.cm⁻³, and coconut trunk was 0.78 and 0.77 g.cm⁻³. The ANOVA results show differences in wood species and significantly affect the value of specific gravity and density. Heartwood pine has a higher specific gravity and density value than sapwood pine. It is related to the thicker cell walls in the heartwood due to the physiological function of wood is dead (Karlinsari et al. 2010).

Table 4. Physical properties of raw material CLT

Characteristics	Pine (Heartwood)	Pine (Sapwood)	Coconut Trunk
Specific Gravity	0.52 ± 0.02 ^a	0.50 ± 0.04 ^a	0.63 ± 0.00 ^b
Density (g.cm ⁻³)			
Air-Dried	0.53 ± 0.08 ^a	0.51 ± 0.06 ^a	0.776 ± 0.08 ^b
Kiln-Dried	0.54 ± 0.07 ^a	0.50 ± 0.06 ^a	0.769 ± 0.07 ^b
Moisture Content (%)	15.35 ± 1.03 ^b	15.98 ± 0.58 ^b	12.646 ± 0.61 ^a
Volume Shrinkage (%)	15.32 ± 1.99 ^b	15.68 ± 0.87 ^b	11.721 ± 1.98 ^a

Notes: Numbers followed by different letters in the same column indicate significant differences in values from the ANOVA results ($\alpha = 0.05$). Data is the average value of $n = 5$.

Moisture content (MC) value of raw material ranged from 12.65-15.98%. The highest MC was found in sapwood pine (15.98%), then followed by heartwood pine (15.35%) and coconut trunk (12.65%). The ANOVA results show that wood species significantly influenced the moisture content value. Based on **Table 4**, pine and coconut still fulfilled the CLT raw material standard of 15% (ANSI 2018). Volumetric shrinkage of raw material ranged from 11.72-15.39%. Volumetric shrinkage of coconut trunk (11.72%) is lower than heartwood pine (15.32%) and sapwood pine (15.40%). The ANOVA results show that the wood species significantly affected moisture content and volume shrinkage value. It is due to the dimension of the coconut trunk being more stable than pine wood. The volumetric shrinkage of heartwood pine is lower than sapwood pine. It is due to higher crystallinity in heartwood than in sapwood (Yuniati et al. 2020).

Table 5 shows the coconut trunk extractive content, higher than pine wood in three solvents. Extractives and pH will affect the wettability and dimensional stability (Bossu et al. 2016; Jankowska et al. 2018; Priadi et al. 2019), so in this study, the dimensions of coconut trunk should be more stable than pine wood. However, extractives can limit adhesive penetration on wood. It is because the wood extractive substances are located in the cell cavity (Sutiya 2012), making wood with high extractives harder for the adhesive to penetrate the wood. In contrast, Lai et al. (2021) discovered that the particle size of PU adhesive is stable at pH 5-12, so pine wood and coconut trunk wettability cannot be affected in this study.

Table 5. Extractive content and pH of raw material CLT

Characteristics	Pine	Coconut trunk
Extractive content (%)		
Dissolved in Room Temperature Water	10.98 ± 0.77 ^a	14.18 ± 1.47 ^b
Dissolved in Hot Water	6.79 ± 0.81 ^a	11.19 ± 0.22 ^b
Dissolved in 1% NaOH	16.60 ± 0.53 ^a	22.72 ± 1.15 ^b
pH	6.05 ± 0.52 ^a	7.36 ± 0.08 ^b

Notes: Numbers followed by different letters in the same column indicate significant differences in values from the ANOVA results ($\alpha = 0.05$). Data is the average value of n = 5.

Table 6 exhibits the higher surface roughness of coconut trunks than pine wood, but the pine wood wettability is higher than coconut trunks. The ANOVA results show that raw material species significantly affected the surface roughness and contact angle value. The adhesion is better on pine wood than the coconut trunk. Adhesive penetrates and fills the wood pores, forming a physical and chemical bond with the wood surface (Darmawan et al. 2018, 2020).

Table 6. Surface characteristics of raw material CLT

Characteristics	Pine	Coconut
Surface Roughness (μm)	5.72 ± 0.57 ^a	11.38 ± 1.76 ^b
Contact Angle ($^\circ$)	24.40 ± 3.25 ^a	32.78 ± 2.12 ^b
Wettability	0.12 ± 0.04 ^a	0.06 ± 0.01 ^a

Notes: Numbers followed by different letters in the same column indicate significant differences in values from the ANOVA results ($\alpha = 0.05$). Data is the average value of n = 5.

Changes in the contact angle of PU 1.8 adhesive on the coconut trunk and pine wood surfaces are shown in **Fig. 6**. The initial contact angle of PU 1.8 droplet on pine wood is slightly lower but decreases sharper than coconut trunk in the first min. It shows that PU 1.8 adhesive can penetrate well on pine wood.

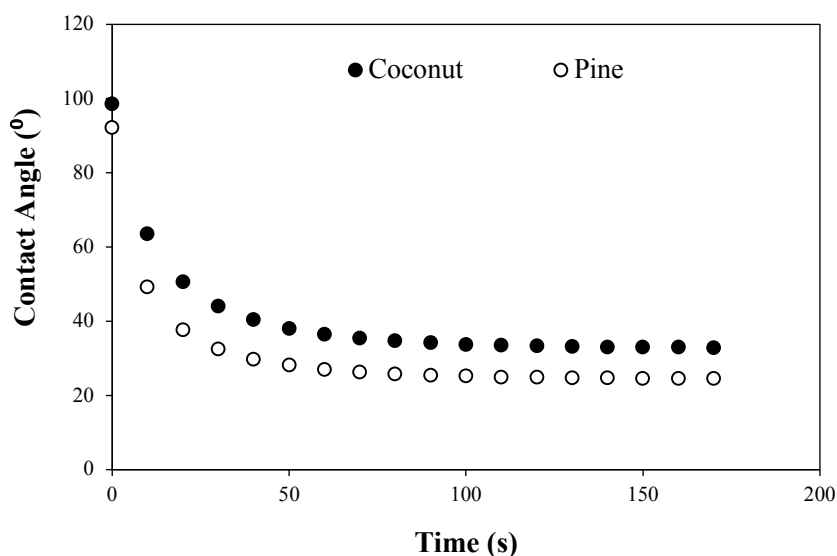


Fig. 6. Changes in contact angle of PU adhesives on time changes in pine wood and coconut trunk.

3.3. Characteristics of Cross-Laminated Timber

The density values of CLT were 0.53-0.71 g.cm⁻³ (**Fig. 7**). Single coconut trunk CLT has the highest density (0.71 g.cm⁻³), and single pine wood CLT has the lowest (0.53 g.cm⁻³). The result of ANOVA showed a significant influence of lamina combination on the CLT density. The DMRT results show that the density values of CLT significantly differed at each level. It is due to the density of the raw material of CLT. Based on **Table 4**, coconut trunk density was higher than pine wood. Srivaro et al. (2021) stated that the higher the raw material density, the higher density of the CLT panel produced.

The values of CLT moisture content ranged from 12.57-16.39% (**Fig. 7**). The highest moisture content was in single pine wood CLT (16.39%), and the lowest was in single coconut trunk CLT (12.57%). Only single coconut trunk CLT met the standard, requiring a moisture content of CLT under 15%. The result of ANOVA showed a significant influence of lamina combination on the CLT moisture content. The DMRT results showed that moisture content CLT values differed significantly at each level. It is related to the moisture content of raw material. **Table 4** shows that the coconut trunk has lower moisture content than pine wood.

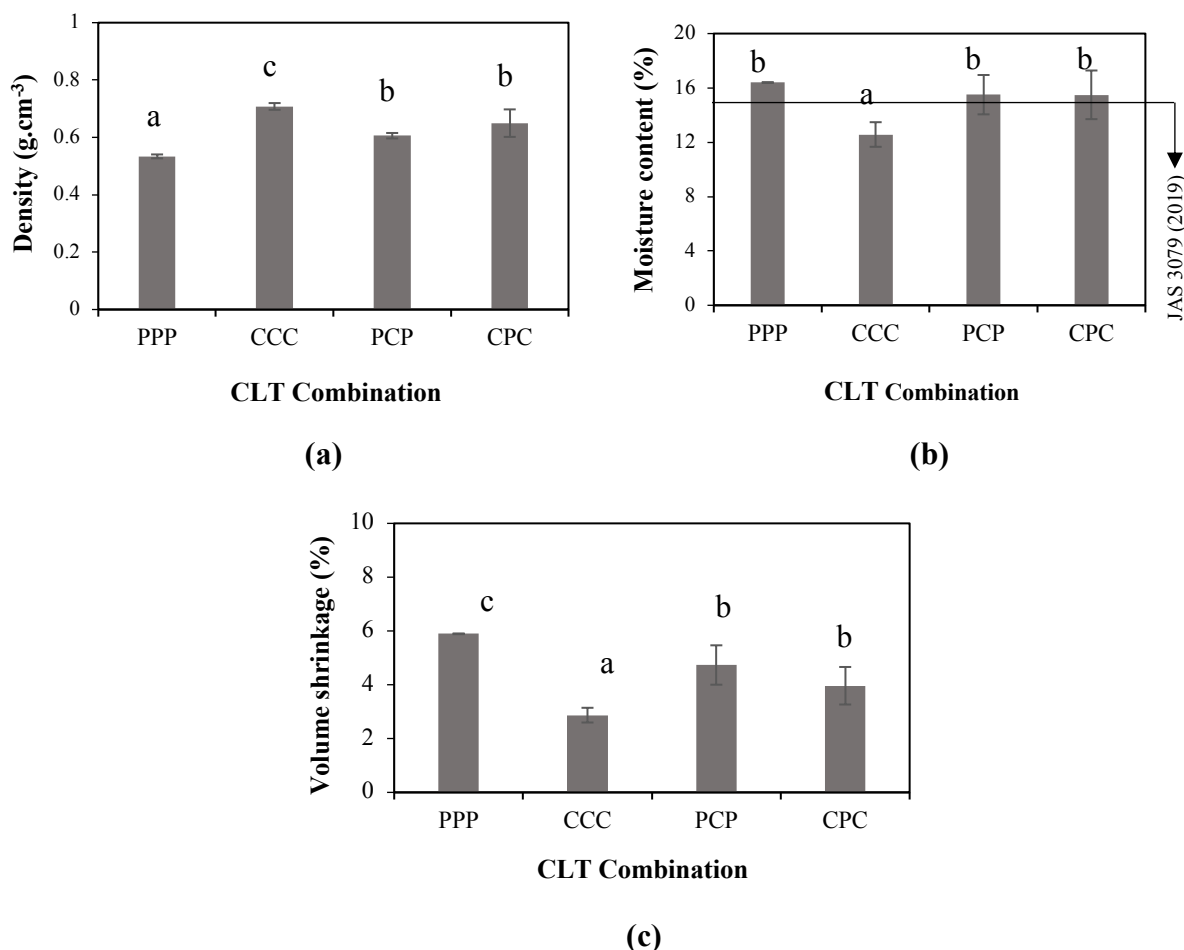


Fig. 7. (a) Density, (b) moisture content, and (c) volume shrinkage values on various layer combinations.

The volume shrinkage values of CLT ranged from 2.87-5.90%. The highest volume shrinkage was found in single pine wood CLT (5.90%), and the lowest was in single coconut trunk CLT (2.87%). The ANOVA showed that the CLT combination significantly affected volume

shrinkage CLT values. The DMRT results showed that the volume shrinkage CLT values differed significantly at each level. Single pine wood CLT has a higher volume shrinkage value than single coconut trunk CLT. It is also related to the volume shrinkage of raw material, which mentioned that pine wood's volume shrinkage is higher than coconut trunk (**Table 4**).

The water adsorption (WA) and thickness swelling (TS) values of CLT ranged from 17.21-38.79% and 3.69-7.15%, respectively (**Fig. 8**). The highest WA was found in single pine wood CLT (38.79%) and the lowest was found in single coconut trunk CLT (17.21%). The highest TS was found in single pine wood CLT (7.15%) and the lowest in single coconut trunk CLT (3.69%).

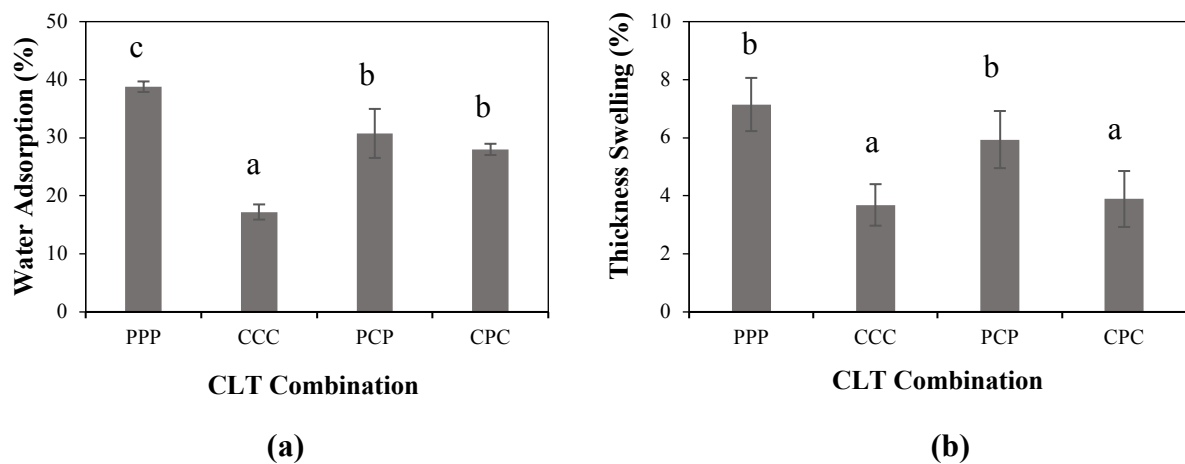


Fig. 8. Water adsorption (a) and thickness swelling (b) values of CLT on various layer combinations.

The result of ANOVA showed that there is a significant influence of lamina combination on the CLT WA and TS. The WA and TS values of CLT were significantly different at each level according to DMRT. Single pine wood CLT has a higher WA and TS than hybrid PCP and CPC CLT. Single coconut trunk CLT has lower WA and TS than hybrid PCP and CPC CLT. It is due to the differences in the raw material density. Pinewood has a lower density than coconut trunk. According to [Glass and Zelinka \(2010\)](#) and [Srivaro et al. \(2021\)](#), low-density wood has higher porosity, so more water penetration occurs. **Table 4** and **Table 5** show that pine wood has higher volume shrinkage, lower density, and lower extractive content than coconut trunk. These values show that coconut has better dimensional stability than pine wood. It means pine wood can be improved when combined with coconut trunks as CLT.

3.3.1. Cold and hot water delamination

The water and boiled water delamination values of CLT are 30.26-72.51% and 26.34-80.18% (**Fig. 9**). The highest water and boiled water delamination value of CLT was found in single coconut CLT (72.51% and 80.18%), and the lowest was in single pine wood CLT (30.26% and 26.34%). The result of ANOVA showed that there is a significant influence of the lamina combination on the CLT cold water and boiled water delamination values. The hybrid CLT PCP and CPC are higher than single pine wood CLT but lower than single coconut trunk CLT. It can be related to the moisture content and wettability of raw material. Based on **Table 4**, the moisture content value of pine wood was higher than the coconut trunk. The wettability of pine wood is higher than the coconut trunk (**Table 6**). It means the adhesives can penetrate well and form chemical bonds in pine wood more than in coconut trunks ([Darmawan et al. 2018, 2020](#)). When

the PU adhesive penetrates, it is easier for the adhesive to form bonds on wood with high moisture content because there are more hydroxyl groups in the wood, so it reacts with the PU adhesive. The CLT bonding quality is determined by specimen form, layer number and thickness, and bonding pressure (Knorz et al. 2017).

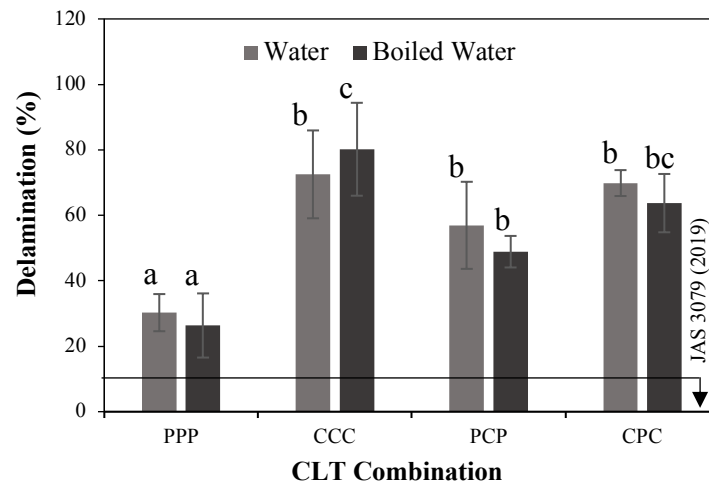


Fig. 9. Water and boiled water delamination values of CLT on various layer combinations.

All CLTs did not meet the CLT standard (JAS 2019), which states the maximum of CLT delamination is 10%. Other CLT delamination investigations have found that CLT bonded with PU adhesive and using different wood species also has a high delamination value. CLT produced from acacia wood had delamination values of 36.29% and 70.80% (Yusof et al. 2019). Polyurethane adhesives bonding caused low delamination resistance (Knorz et al. 2014). It can be acceptable because the adhesive cannot penetrate well into the material, especially the coconut trunk, which has the highest physical and chemical properties. According to Widyorini et al. (2014), heat pretreatment (oven and steam method) on raw material with a temperature of 160°C for 3 h can decrease the delamination value. It is due to heat pretreatment improving dimensional stability. Wood improvement in dimensional stability, in general, will increase the adhesive properties because it will reduce the shrinkage of the glued wood so that the shrinkage does not easily damage the adhesive line.

3.3.2. MOE and MOR

Fig. 10 shows the MOE value (a) and MOR value (b) on every sample of CLT. The MOE CLT values obtained ranged from 16831.01 to 26512.31 MPa (**Fig. 10a**). The lowest MOE value is in the PPP CLT, and the highest is in the CPC CLT. The analysis of variance (ANOVA) showed that the combination of layers significantly affected the MOE value of CLT. CLT MOR values ranged from 26.59 to 39.62 MPa (**Fig. 10b**). The lowest MOR value is in the PCP CLT, and the highest is in the KKK CLT. The result of ANOVA showed that there is a significant influence of lamina combination on the CLT MOR value. The MOE and MOR values differed significantly at each level according to DMRT.

The MOE value of pine hybrid CLT was higher than that of single pine CLT. The MOE value of CLT KPK was higher than single coconut CLT. It is consistent with prior research that found hybrid CLTs to have better mechanical characteristics than single CLTs (Aicher et al. 2016; Corpataux et al. 2020; Hematabadi et al. 2020). Improvement of mechanical properties using dual

species on composite panels has also been reported (Maulana et al. 2021). Meanwhile, the MOR value of hybrid pine and coconut CLT has a lower value than the CLT of single pine and coconut. It can be caused by the damage from the adhesive line, which is related to the delamination value (Fig. 9). In addition, the properties of the two wood species impact the quality of the CLT. Coconut tends to be better quality than pine wood (Table 4-6). Therefore, CLT composed of coconut wood had higher MOE and MOR values than CLT composed of pine wood. The MOE value of pine wood is 8900 MPa, and for coconut is 6381 MPa, while the MOR for pine wood is 71 MPa and for coconut is 52 MPa (Lestari et al. 2017; Srivaro et al. 2020). The MOE value of CLT was higher than the solid wood, while the MOR value of CLT was lower than the solid wood (Fig. 10). This is due to the adhesive link in CLT (Mardikanto et al. 2017).

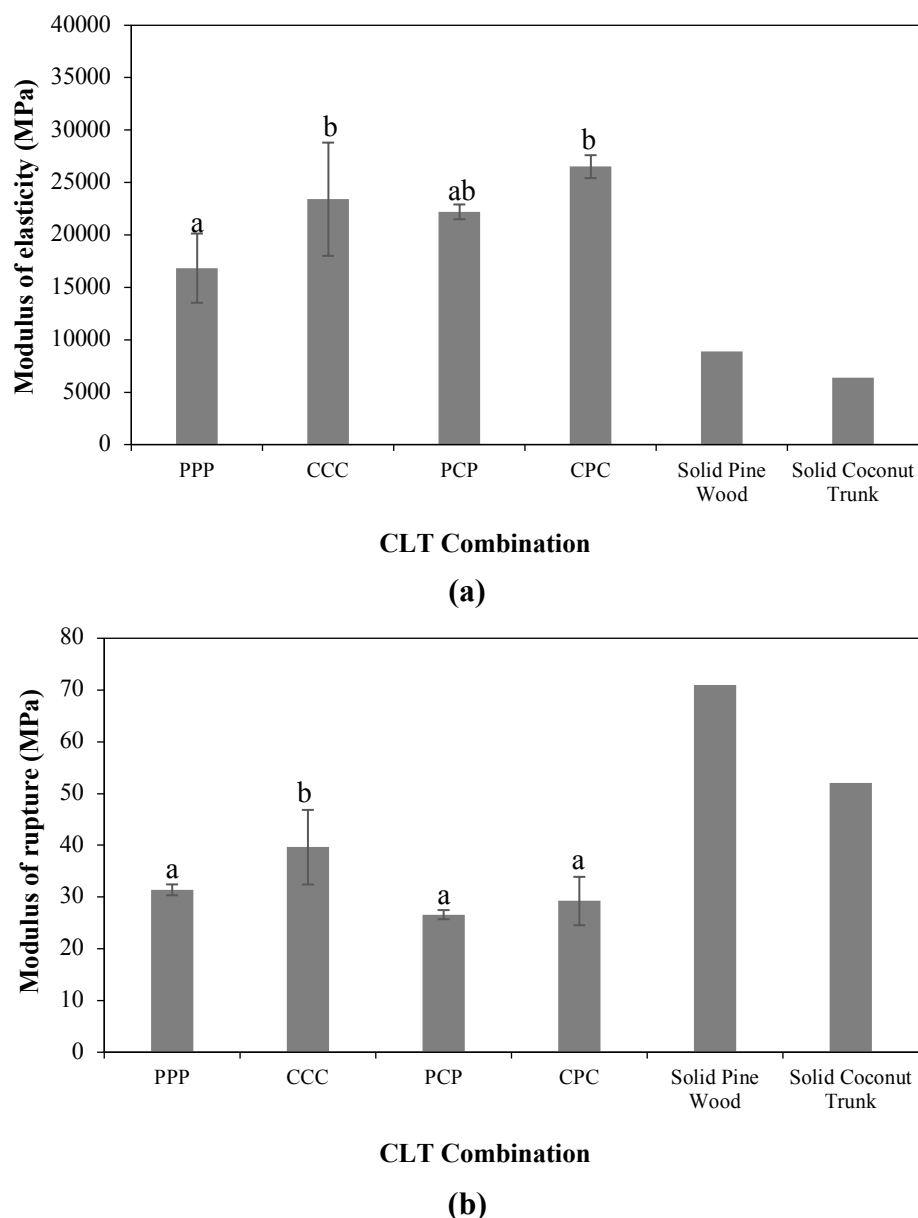


Fig. 10. MOE (a) and MOR (b) values of CLT on various layer combinations.

3.3.3. Shear strength

Fig. 11 exhibits shear strength values of CLT parallel to grain of 1.23-2.63 MPa and perpendicular to grain shear strength of 0.43-1.27 MPa. Single pine wood CLT shear strength has

the highest value in parallel (2.63 MPa) and perpendicular (1.27 MPa) to grain. Single coconut CLT has the lowest shear strength in parallel (1.23 MPa) and perpendicular (0.43 MPa) to grain.

The result of ANOVA showed that there is a significant influence of lamina on the CLT parallel and perpendicular-to-grain shear strength. The DMRT results showed that the parallel and perpendicular to grain shear strength values differed significantly at each level. The shear strength values of single pine wood CLT are better than single coconut trunk CLT. It means the hybrid and the coconut are not suitable to be made as CLT.

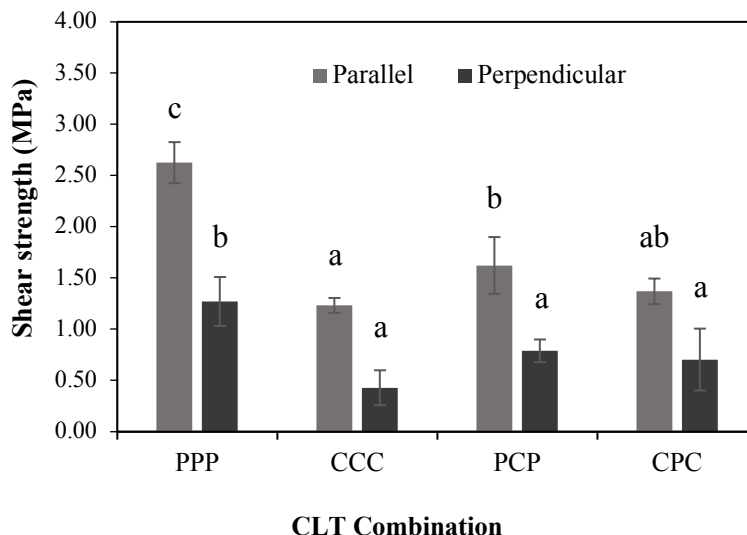


Fig. 11. Parallel and perpendicular to grain shear strength values of CLT on various layer combinations.

The shear strength value of CLT is negatively correlated with the delamination value. The higher delamination value causes the lower shear strength. Based on **Fig. 9**, single pine wood CLT has the lowest delamination. It can cause the single pine wood CLT to have the highest shear strength value. It is because pine wood density is lower than coconut trunk. Higher-density material had a more difficult bonding performance (Lu et al. 2018).

The shear strength value of CLT is stated with a minimum percentage of 90% (JAS 3079:2019). **Table 7** exhibits the damage results analysis of the shear strength test. On average, all samples did not fulfill the JAS 3079 (2019) standard. However, the individual samples contained CLT that met the standard. A total of 1 sample of single pine wood CLT and 1 sample of CLT CPC in the shear strength test perpendicular of grain had a percentage of wood damage of 100%. No CLT sample has wood damage of 100% in the shear strength test parallel to the grain.

Table 7. The wood failure percentage value of CLT

Layer combination of CLT	WFP (JAS 3079:2019 (≥ 90%))	
	Shear strength parallel to the grain	Shear strength perpendicular to the grain
PPP	29.60	33.33
CCC	38.25	8.11
PCP	6.71	44.36
CPC	37.74	33.33

4. Conclusions

The polyurethane (PU) adhesive had a solid content of 97.37%, gel time was 84.9 min, viscosity at each rotation speed was 784.96 mPa.s (50/s), 869.92 mPa.s (100/s), 947.67 mPa.s (150/s). Analysis of the FTIR functional group and analysis of Py-GCMS showed the spectra of the presence of –NCO and –OH bonds. The results of the DMA test showed that at a temperature of 27.93°C, the highest storage modulus value is obtained. Testing the attributes of cross-laminated timber (CLT) wood material found that pine and coconut had distinct physical and chemical properties but had similar wettability to polyurethane adhesives. The results of statistical analysis of the CLT test showed a significant effect of layer combination on density, moisture content, shrinkage volume, water absorption, thickness swelling, delamination, and shear strength. None of the CLTs met the JAS 3079 (2019) standard for delamination ($\leq 10\%$) and wood failure ($\geq 90\%$). The overall test results show that the hybrid PCP CLT has better density, moisture content, volume shrinkage, water adsorption, thickness swelling, delamination, and MOE values than single pine wood CLT. In contrast, single coconut trunk CLT has better density, moisture content, volume shrinkage, water adsorption, thickness swelling, and MOR values than hybrid CPC CLT. Research about pretreatment (i.e., heat pretreatment) of pine and coconut trunks should be done to improve the characteristic of CLT's raw material. However, it is also necessary to pay attention to the reactivity of the wood with the adhesive used so that the results are optimal.

Acknowledgements

This research was conducted as part of the Riset dan Inovasi untuk Indonesia Maju (RIIM) project Number 65/II.7/HK/2022. This study was also supported by The National Research and Innovation Agency (BRIN), Indonesia, grant Number 3/III.10/HK/2023.

References

- Aicher, S., Hirsch, M., and Christian, Z. 2016. Hybrid Cross-Laminated Timber Plates with Beech Wood Cross-Layers. *Construction and Building Materials* 124: 1007–1018. DOI: [10.1016/j.conbuildmat.2016.08.051](https://doi.org/10.1016/j.conbuildmat.2016.08.051)
- Aisyah, S., Hadi, Y. S., Lubis, M. A. R., Maulana, M. I., Sari, R. K., and Hidayat, W. 2023. Influence of Puspa Wood and Coconut Trunk Combination on the Characteristics of Cross-Laminated Timber Bonded with Polyurethane Adhesive. *Jurnal Sylva Lestari* 11(1): 136–162. DOI: [10.23960/jsl.v11i1.647](https://doi.org/10.23960/jsl.v11i1.647)
- ANSI. 2018. *ANSI/APA PRG 320-2018: Standard for Performance-Rated Cross-Laminated Timber*. The Engineered Wood Association (APA) 40. Tacoma, Washington, USA.
- ASTM. 2014. Standard Test Methods for Small Clear Specimens of Timber - D143. *ASTM International* 31. DOI: [10.1520/d0143-14.2](https://doi.org/10.1520/d0143-14.2)
- Awaludin, A., and Sutapa, J. P. G. 2017. Mechanical Properties of *Cocos nucifera* Wood Planted Around Mt. Merapi, Yogyakarta. *Wood Research Journal* 3(1): 6–10. DOI: [10.51850/wrj.2012.3.1.6-10](https://doi.org/10.51850/wrj.2012.3.1.6-10)
- Bahmanzad, A., Clouston, P. L., Arwade, S. R., and Schreyer, A. C. 2020. Shear Properties of Eastern Hemlock with Respect to Fiber Orientation for Use in Cross Laminated Timber. *Journal of Materials in Civil Engineering* 32(7): 1–11. DOI: [10.1061/\(asce\)mt.1943-5533.0003232](https://doi.org/10.1061/(asce)mt.1943-5533.0003232)

- Bekhta, P., Sedliačik, J., and Bekhta, N. 2020. Effects of Selected Parameters on the Bonding Quality and Temperature Evolution Inside Plywood during Pressing. *Polymers* 12(5): 3–8. DOI: [10.3390/polym12051035](https://doi.org/10.3390/polym12051035)
- Böhning, M., Frasca, D., Schulze, D., and Schartel, B. 2019. Multilayer Graphene/Elastomer Nanocomposites. in: *Carbon-Based Nanofillers and Their Rubber Nanocomposites: Fundamentals and Applications*. Elsevier, Berlin, Germany 139–200. DOI: [10.1016/b978-0-12-817342-8.00006-8](https://doi.org/10.1016/b978-0-12-817342-8.00006-8)
- Bossu, J., Beauchêne, J., Estevez, Y., Duplais, C., and Clair, B. 2016. New Insights on Wood Dimensional Stability Influenced by Secondary Metabolites: The Case of a Fast-Growing Tropical Species *Bagassa guianensis* Aubl. *PLoS ONE* 11(3): e0150777. DOI: [10.1371/journal.pone.0150777](https://doi.org/10.1371/journal.pone.0150777)
- Brandner, R., Flatscher, G., Ringhofer, A., Schickhofer, G., and Thiel, A. 2016. Cross Laminated Timber (CLT): Overview and Development. *European Journal of Wood and Wood Products* 74(3): 331–351. DOI: [10.1007/s00107-015-0999-5](https://doi.org/10.1007/s00107-015-0999-5)
- Corpataux, L., Okuda, S., and Kua, H. W. 2020. Panel and Plate Properties of Cross-Laminated Timber (CLT) with Tropical Fast-Growing Timber Species in Compliance with Eurocode 5. *Construction and Building Materials* 261: 119672. DOI: [10.1016/j.conbuildmat.2020.119672](https://doi.org/10.1016/j.conbuildmat.2020.119672)
- Darmawan, W., Ginting, M. B., Gayatri, A., Putri, R. L., Lumongga, D., and Hasanusi, A. 2020. Influence of Surface Roughness of Ten Tropical Woods Species on Their Surface Free Energy, Varnishes Wettability and Bonding Quality. *Pigment and Resin Technology* 49(6): 441–447. DOI: [10.1108/prt-01-2020-0005](https://doi.org/10.1108/prt-01-2020-0005)
- Darmawan, W., Nandika, D., Noviyanti, E., Alipraja, I., Lumongga, D., Gardner, D., and Gérardin, P. 2018. Wettability and Bonding Quality of Exterior Coatings on Jabon and Sengon Wood Surfaces. *Journal of Coatings Technology and Research* 15(1): 95–104. DOI: [10.1007/s11998-017-9954-1](https://doi.org/10.1007/s11998-017-9954-1)
- Dyer, E., and Newborn, G. E. 1958. Thermal Degradation of Carbamates of Methylenebis-(4-phenyl Isocyanate). *Journal of the American Chemical Society* 80(20): 5495–5498. DOI: [10.1021/ja01553a045](https://doi.org/10.1021/ja01553a045)
- Dyer, E., and Read, R. E. 1961. Thermal Degradation of O-1-Hexadecyl N-1-Naphthylcarbamates and Related Compounds. *Journal of Organic Chemistry* 26(11): 4388–4394. DOI: [10.1021/jo01069a050](https://doi.org/10.1021/jo01069a050)
- Dyer, E., and Wright, G. C. 1959. Thermal Degradation of Alkyl N-Phenylcarbamates. *Journal of the American Chemical Society* 81(9): 2138–2143. DOI: [10.1021/ja01518a030](https://doi.org/10.1021/ja01518a030)
- Febrianto, F., Hidayat, W., Kim, J. H., and Kim, N. H. 2021. *Guidebook for Species Identification and Effective Utilization of Tropical Woods*. IPB Press.
- Glass, S. V., and Zelinka, S. L. 2010. Wood Handbook, Chapter 04: Moisture Relations and Physical Properties of Wood. *Wood handbook: Wood as An Engineering Material* (GTR-190): 1–19.
- Gurunathan, T., Mohanty, S., and Nayak, S. K. 2015. Isocyanate Terminated Castor Oil-Based Polyurethane Prepolymer: Synthesis and Characterization. *Progress in Organic Coatings* 80: 39–48. DOI: [10.1016/j.porgcoat.2014.11.017](https://doi.org/10.1016/j.porgcoat.2014.11.017)
- Hadjib, N., and Rachman, O. 2009. Daur Teknis Pinus Tanaman untuk Kayu Pertukangan Berdasar Sifat Fisis dan Mekanis. *Jurnal Penelitian Hasil Hutan* 27(1): 76–87. DOI: [10.20886/jphh.2009.27.1.76-87](https://doi.org/10.20886/jphh.2009.27.1.76-87)

- Handika, S.O., Lubis, M.A.R., Sari, R.K., Laksana, R.P.B., Antov, P., Savov, V., Gajtanska, M. and Iswanto, A.H., 2021. Enhancing Thermal and Mechanical Properties of Ramie Fiber via Impregnation by Lignin-Based Polyurethane Resin. *Materials* 14(22): 6850-6877. DOI: [10.3390/ma14226850](https://doi.org/10.3390/ma14226850)
- Hariz, T. M. R., Hadi, Y. S., Lubis, M. A. R., Maulana, M. I., Sari, R. K., and Hidayat, W. 2023. Physical and Mechanical Properties of Cross-Laminated Timber Made of a Combination of Mangium-Puspa Wood and Polyurethane Adhesive. *Jurnal Sylva Lestari* 11(1): 37–65. DOI: [10.23960/jsl.v11i1.645](https://doi.org/10.23960/jsl.v11i1.645)
- Hasburgh, L., Bourne, K., Peralta, P., Mitchell, P., Schiff, S., and Pang, W. 2016. *Effect of Adhesives and Ply Configuration on the Fire Performance of Southern Pine Cross-Laminated Timber*. WCTE 2016 - World Conference on Timber Engineering, Vienna, Austria.
- Hass, P., Wittel, F. K., Mendoza, M., Herrmann, H. J., and Niemz, P. 2012. Adhesive Penetration in Beech Wood: Experiments. *Wood Science and Technology* 46(1–3): 243–256. DOI: [10.1007/s00226-011-0410-6](https://doi.org/10.1007/s00226-011-0410-6)
- Hazmi, A. S. A., Aung, M. M., Abdullah, L. C., Salleh, M. Z., and Mahmood, M. H. 2013. Producing Jatropha Oil-Based Polyol via Epoxidation and Ring Opening. *Industrial Crops and Products* 50: 563–567. DOI: [10.1016/j.indcrop.2013.08.003](https://doi.org/10.1016/j.indcrop.2013.08.003)
- Hematabadi, H., Madhoushi, M., Khazaeyan, A., Ebrahimi, G., Hindman, D., and Loferski, J. 2020. Bending and Shear Properties of Cross-Laminated Timber Panels Made of Poplar (*Populus alba*). *Construction and Building Materials* 265: 120326. DOI: [10.1016/j.conbuildmat.2020.120326](https://doi.org/10.1016/j.conbuildmat.2020.120326)
- Hidayat, W., Aprilliana, N., Asmara, S., Bakri, S., Hidayati, S., Banuwa, I.S., Lubis, M.A.R. and Iswanto, A.H., 2022. Performance of Eco-Friendly Particleboard from Agro-Industrial Residues Bonded with Formaldehyde-Free Natural Rubber Latex Adhesive for Interior Applications. *Polymer Composites* 43(4): 2222-2233. DOI: [10.1002/pc.26535](https://doi.org/10.1002/pc.26535)
- Indrosaptono, D., Sukawi, S., and Indraswara, M. S. 2018. Kayu Kelapa (Glugu) sebagai Alternatif Bahan Konstruksi Bangunan. *MODUL* 14(1): 53–58. DOI: [10.14710/mdl.14.1.2014.53-58](https://doi.org/10.14710/mdl.14.1.2014.53-58)
- Jankowska, A., Boruszewski, P., Drozddek, M., Rębkowski, B., Kaczmarczyk, A., and Skowrońska, A. 2018. The Role of Extractives and Wood Anatomy in the Wettability and Free Surface Energy of Hardwoods. *BioResources* 13(2): 3082–3097. DOI: [10.15376/biores.13.2.3082-3097](https://doi.org/10.15376/biores.13.2.3082-3097)
- JAS. 2019. *Jas 3079: Cross Laminated Timber*. Ministry of Agriculture, Forestry, and Fisheries, Tokyo.
- Karacabeyli, E., and Douglas, B. 2013. *Hand Book Cross Laminated Timber*. Book. FPInnovations. Leesburg.
- Karlinasari, L., Nawawi, D., and Widayani, M. 2010. Kajian Sifat Anatomi dan Kimia Kayu Kaitannya dengan Sifat Akustik Kayu. *Jurnal Ilmu-Ilmu Hayati Dan Fisik* 12(3): 110–116.
- Knorz, M., Schmidt, M., Torno, S., and Van De Kuilen, J. W. 2014. Structural Bonding of Ash (*Fraxinus excelsior* L.): Resistance to Delamination and Performance in Shearing Tests. *European Journal of Wood and Wood Products* 72(3): 297–309. DOI: [10.1007/s00107-014-0778-8](https://doi.org/10.1007/s00107-014-0778-8)
- Knorz, M., Torno, S., and van de Kuilen, J. W. 2017. Bonding Quality of Industrially Produced Cross-Laminated Timber (CLT) as Determined in Delamination Tests. *Construction and Building Materials* 133: 219–225. DOI: [10.1016/j.conbuildmat.2016.12.057](https://doi.org/10.1016/j.conbuildmat.2016.12.057)

- Kong, X., Liu, G., and Curtis, J. M. 2011. Characterization of Canola Oil Based Polyurethane Wood Adhesives. *International Journal of Adhesion and Adhesives* 31(6): 559–564. DOI: [10.1016/j.ijadhadh.2011.05.004](https://doi.org/10.1016/j.ijadhadh.2011.05.004)
- Kusyanto, M. 2015. Kajian Material Kayu Glugu Sebagai Bahan Bangunan. *Jurnal Teknik UNISFAT* 10(2): 33–44.
- Lai, Y., Qian, Y., Yang, D., Qiu, X., and Zhou, M. 2021. Preparation and Performance of Lignin-Based Waterborne Polyurethane Emulsion. *Industrial Crops and Products* 170(6): 113739. DOI: [10.1016/j.indcrop.2021.113739](https://doi.org/10.1016/j.indcrop.2021.113739)
- Lei, H., and Frazier, C. E. 2015. A Dynamic Mechanical Analysis Method for Predicting the Curing Behavior of Phenol-Formaldehyde Resin Adhesive. *Journal of Adhesion Science and Technology* 29(10): 981–990. DOI: [10.1080/01694243.2015.1011735](https://doi.org/10.1080/01694243.2015.1011735)
- Lestari, R. Y. 2017. CLT (Cross Laminated Timber): Production, Characteristics and Development. *Jurnal Riset Industri Hasil Hutan* 9(1): 41–55. DOI: [10.24111/jrihh.v9i1.3126](https://doi.org/10.24111/jrihh.v9i1.3126)
- Liao, Y., Tu, D., Zhou, J., Zhou, H., Yun, H., Gu, J., and Hu, C. 2017. Feasibility of Manufacturing Cross-Laminated Timber using Fast-Grown Small Diameter Eucalyptus Lumbers. *Construction and Building Materials* 132: 508–515. DOI: [10.1016/j.conbuildmat.2016.12.027](https://doi.org/10.1016/j.conbuildmat.2016.12.027)
- Lu, Z., Zhou, H., Liao, Y., and Hu, C. 2018. Effects of Surface Treatment and Adhesives on Bond Performance and Mechanical Properties of Cross-Laminated Timber (CLT) Made from Small Diameter Eucalyptus Timber. *Construction and Building Materials* 161: 9–15. DOI: [10.1016/j.conbuildmat.2017.11.027](https://doi.org/10.1016/j.conbuildmat.2017.11.027)
- Lubis, M. A. R., Labib, A., Sudarmanto, Akbar, F., Nuryawan, A., Antov, P., Kristak, L., and Papadopoulos, A. N. 2022. Influence of Lignin Content and Pressing Time on Plywood Properties Bonded with Cold-Setting Adhesive Based on Poly (Vinyl Alcohol), Lignin, and Hexamine. *Polymers* 14(10). DOI: [10.3390/polym14102111](https://doi.org/10.3390/polym14102111)
- Mardikanto, T., Karlina, L., and Bahtiar, E. 2017. *Sifat Mekanis Kayu*. IPB Press, Bogor.
- Marko, G., Bejo, L., and Takats, P. 2016. Cross-Laminated Timber Made of Hungarian Raw Materials. *IOP Conference Series: Materials Science and Engineering* 123(1): 012059. DOI: [10.1088/1757-899x/123/1/012059](https://doi.org/10.1088/1757-899x/123/1/012059)
- Maulana, S., Hidayat, W., Sumardi, I., Wistara, N. J., Maulana, M. I., Kim, J. H., Lee, S. H., Kim, N. H., and Febrianto, F. 2021. Properties of Dual-Species Bamboo-Oriented Strand Boards Bonded with Phenol Formaldehyde Adhesive under Various Compression Ratios. *BioResources* 16(3): 5422–5435. DOI: [10.15376/biores.16.3.5422-5435](https://doi.org/10.15376/biores.16.3.5422-5435)
- Menard, K. P., and Menard, N. R. 1990. *Dynamic Mechanical Analysis*. American Chemical Society, Polymer Preprints, Division of Polymer Chemistry. DOI: [10.3139/9781569906446.012](https://doi.org/10.3139/9781569906446.012)
- Oliviero, M., Stanzione, M., D’Auria, M., Sorrentino, L., Iannace, S., and Verdolotti, L. 2019. Vegetable Tannin as a Sustainable UV Stabilizer for Polyurethane Foams. *Polymers* 11(3): 1–16. DOI: [10.3390/polym11030480](https://doi.org/10.3390/polym11030480)
- Park, B. D., and Kim, J. W. 2008. Dynamic Mechanical Analysis of Urea–Formaldehyde Resin Adhesives with Different Formaldehyde-to-Urea Molar Ratios. *Journal of Applied Polymer Science* 108(3): 2045–2051. DOI: [10.1002/app](https://doi.org/10.1002/app)
- Poh, A. K., Sin, L. C., Foon, C. S., and Hock, C. C. 2014. Polyurethane Wood Adhesive from Palm Oil-Based Polyester Polyol. *Journal of Adhesion Science and Technology* 28(11):

- 1020–1033. DOI: [10.1080/01694243.2014.883772](https://doi.org/10.1080/01694243.2014.883772)
- Polosakan, R., and Alhamd, L. 2014. Estimasi Biomasa dan Karbon Tersimpan pada *Pinus merkusii* Jungh. & De Vriese di Hutan Pinus Gn. Bunder, Tn. Gn. Halimun Salak. *Berita Biologi* 13(4): 115–120.
- Priadi, T., Sholihah, M., and Karlinasari, L. 2019. Water Absorption and Dimensional Stability of Heat-Treated Fast-Growing Hardwoods. *Journal of the Korean Wood Science and Technology* 47(5): 567–578. DOI: [10.5658/wood.2019.47.5.567](https://doi.org/10.5658/wood.2019.47.5.567)
- Rangkang, J. 2016. Karakteristik Kayu Kelapa di Berbagai Zona di Indonesia Timur Berdasarkan Sifat Fisis dan Mekanisnya. *Jurnal Teknik Sipil* 23(2): 89–98.
- Sanjaya, W. A., and Tobing, R. R. 2019. Rumah Susun Modular dengan Pemanfaatan Papan Prefabrikasi CLT, Kasus : Rumah Susun Siwalankerto, Surabaya. *ARTEKS Jurnal Teknik Arsitektur* 3(2): 199. DOI: [10.30822/artk.v3i2.168](https://doi.org/10.30822/artk.v3i2.168)
- Sankar, M. R., Jain, V. K., Ramkumar, J., and Joshi, Y. M. 2011. Rheological Characterization of Styrene-Butadiene Based Medium and Its Finishing Performance using Rotational Abrasive Flow Finishing Process. *International Journal of Machine Tools and Manufacture* 51(12): 947–957. DOI: [10.1016/j.ijmachtools.2011.08.012](https://doi.org/10.1016/j.ijmachtools.2011.08.012)
- Shi, S. Q., and Gardner, D. J. 2001. Dynamic Adhesive Wettability of Wood. *Wood and Fiber Science* 33(1): 58–68.
- Sikora, K. S., McPolin, D. O., and Harte, A. M. 2016. Shear Strength and Durability Testing of Adhesive Bonds in Cross-Laminated Timber. *Journal of Adhesion* 92(7–9): 758–777. DOI: [10.1080/00218464.2015.1094391](https://doi.org/10.1080/00218464.2015.1094391)
- Srivaro, S., Pásztor, Z., Le Duong, H. A., Lim, H., Jantawee, S., and Tomad, J. 2021. Physical, Mechanical and Thermal Properties of Cross Laminated Timber Made with Coconut Wood. *European Journal of Wood and Wood Products* 79(6): 1519–1529. DOI: [10.1007/s00107-021-01741-y](https://doi.org/10.1007/s00107-021-01741-y)
- Srivaro, S., Tomad, J., Shi, J., and Cai, J. 2020. Characterization of Coconut (*Cocos nucifera*) Trunk's Properties and Evaluation of Its Suitability to be Used as Raw Material for Cross Laminated Timber Production. *Construction and Building Materials* 254: 119291. DOI: [10.1016/j.conbuildmat.2020.119291](https://doi.org/10.1016/j.conbuildmat.2020.119291)
- Sunija, A. J., Ilango, S. S., and Kumar, K. P. V. 2014. Synthesis and Characterization of Bio-Based Polyurethane from Benzoylated Cashewnut Husk Tannins. *Bulletin of Materials Science* 37(3): 735–741. DOI: [10.1007/s12034-014-0665-2](https://doi.org/10.1007/s12034-014-0665-2)
- Sur, S., and Rothstein, J. 2018. Drop Breakup Dynamics of Dilute Polymer Solutions: Effect of Molecular Weight, Concentration, and Viscosity. *Journal of Rheology* 62(5): 1245–1259. DOI: [10.1122/1.5038000](https://doi.org/10.1122/1.5038000)
- Sutiya, B. 2012. Kandungan Kimia dan Sifat Serat Alang-Alang (*Imperata cylindrica*) sebagai Gambaran Bahan Baku Pulp dan Kertas. *Bioscientiae* 9(1): 8–19. DOI: [10.20527/b.v9i1.2583](https://doi.org/10.20527/b.v9i1.2583)
- TAPPI. 1991. *TAPPI Test Methods*. Atlanta.
- Thébault, M., Pizzi, A., Essawy, H. A., Barhoum, A., and Van Assche, G. 2015. Isocyanate Free Condensed Tannin-Based Polyurethanes. *European Polymer Journal* 67: 513–526. DOI: [10.1016/j.eurpolymj.2014.10.022](https://doi.org/10.1016/j.eurpolymj.2014.10.022)
- UNECE/FAO. 2020. *Annual Market Review 2019-2020 - Forest Products*. United Nations Publication.
- Wang, Z., Fu, H., Gong, M., Luo, J., Dong, W., Wang, T., and Chui, Y. H. 2017. Planar Shear and

- Bending Properties of Hybrid CLT Fabricated with Lumber and LVL. *Construction and Building Materials* 151: 172–177. DOI: [10.1016/j.conbuildmat.2017.04.205](https://doi.org/10.1016/j.conbuildmat.2017.04.205)
- Widyorini, R., Khotimah, K., and Prayitno, T. A. 2014. Pengaruh Suhu dan Metode Perlakuan Panas terhadap Sifat Fisika dan Kualitas Finishing Kayu Mahoni. *Jurnal Ilmu Kehutanan* 8(2): 65–74.
- Wijayanti, R. 2014. Perancangan Mebel Repetisi Garis dengan Sistem Lipat dari Kayu Kelapa. *Dimensi Interior* 12(2): 65–71. DOI: [10.9744/interior.12.2.65-71](https://doi.org/10.9744/interior.12.2.65-71)
- Yuniati, A. D., Syahidah, Agussalim, and Suhasman. 2020. *Buku Ajar Ilmu Kayu*. Fakultas Kehutanan Universitas Hasanuddin, Makassar.
- Yusof, N. M., Md Tahir, P., Lee, S. H., Khan, M. A., and Mohammad Suffian James, R. 2019. Mechanical and Physical Properties of Cross-Laminated Timber Made from *Acacia mangium* Wood as Function of Adhesive Types. *Journal of Wood Science* 65: 20. DOI: [10.1186/s10086-019-1799-z](https://doi.org/10.1186/s10086-019-1799-z)
- Zhang, Y., Xia, Z., Huang, H., and Chen, H. 2009. A Degradation Study of Waterborne Polyurethane Based on TDI. *Polymer Testing* 28(3): 264–269. DOI: [10.1016/j.polymeresting.2008.12.011](https://doi.org/10.1016/j.polymeresting.2008.12.011)
- Zhou, J., Chui, Y. H., Niederwestberg, J., and Gong, M. 2020. Effective Bending and Shear Stiffness of Cross-Laminated Timber by Modal Testing: Method Development and Application. *Composites Part B: Engineering* 198(6): 108225. DOI: [10.1016/j.compositesb.2020.108225](https://doi.org/10.1016/j.compositesb.2020.108225)